# Electron structure of excited configurations in $Ca_2V_2O_7$ studied by electron-induced core-ionization loss spectroscopy, appearance-potential spectroscopy, and x-ray-photoelectron spectroscopy

I. M. Curelaru and K. -G. Strid

*Department of Physics, Chalmers University of Technology, S-412 96 Goteborg, Sweden*

E. Suoninen and E. Minni

*Department of Physical Sciences, University of Turku, 20500 Turku, Finland*

T. Rönnhult

*Department of Engineering Materials, Chalmers University of Technology, S-412 96 Goteborg, Sweden*

(Received 11 September 1980)

We have measured the electron-induced core-ionization loss (CILS) spectra, the appearance-potential (APS) spectra, and the x-ray-photoelectron (XPS) spectra of $Ca_2V_2O_7$, that is a prototype for a series of luminescent materials with general formula $M_2V_2O_7$ ($M$ = Mg, Ca, Sr, Ba, Zn, Cd, Hg). From the analysis of the data provided by the edge spectroscopies (CILS and APS) and their comparison with the XPS binding energies, we deduced the electronic structure of the outer orbitals (occupied and empty) involved in these processes. Our data illustrate the strong many-body effects that occur in the excitation and decay of localized atomiclike configurations within the big ionic cluster $V_2O_7^{4-}$. Excitation of core levels in calcium, outside the $V_2O_7^{4-}$ ion, seems to involve more extended orbitals, since the screening is more efficient. Usefulness of complementary studies by x-ray emission and Auger electron spectroscopy is anticipated.

## I. INTRODUCTION

Among the spectroscopic methods for studies of the electron structure of solids, electron-excited core-ionization loss spectroscopy (CILS) and appearance-potential spectroscopy (APS) are good candidates, since they probe in different specific ways the structure of the lowest empty states above the Fermi level. In CILS, at high enough incident energy, the near-edge intensity of the inelastically scattered electrons is proportional to the convolution of the density of empty states of the target material with a broadening function (which can be assumed to be Lorentzian) due to the finite lifetime of the created core hole.[1] In APS, the measured total soft x-ray emission yield resulting from the decay of the excited state is proportional to the self-convolution of the distribution of empty states, folded again by the same core-level broadening function.[2]

CILS is close to x-ray absorption spectroscopy (XAS), and the spectra appear as an edge singularity followed by a broad distribution extended down to zero. In both cases the final state consists of one core hole and one electron near the Fermi level. The main difference between CIS and XAS arises from the selection rules that operate in photon absorption and are absent in electron scattering processes. The fine structure possibly revealed by XAS is thus absent in CILS, but the global information on the distribution of conduction states is expected to be similar.

In APS, the excited system consists of one core hole and two electrons accommodated on the same or on different available states near the Fermi level.

The present work is part of a larger project devoted to the study of the electron structure of a series of vanadate compounds by using various electronic and x-ray spectroscopies. We are interested in vanadium-oxygen compounds in which vanadium is tetrahedrally coordinated to oxygen forming rigid ionic clusters such as $VO_4^{3-}$ (in $MVO_4$, $M$ = Y, Ce, Nd, Eu, Tb, Dy, Gd, Yb) or $V_2O_7^{4-}$ (in $M_2V_2O_7$, $M$ = Mg, Ca, Sr, Ba, Zn, Cd, Hg). The compounds $YVO_4$ and $Ca_2V_2O_7$ chosen by us as prototypes of these materials have luminescent properties and are largely applied as, e.g., coatings in luminescent lamps and color television tubes.[3]

Because of the complicated crystal structure of these compounds, detailed band structure calculations have not been performed. The similarity of the excitation and emissions luminescent spectra within these series of isostructural compounds suggests that vanadate cluster ions alone are responsible for the luminescent properties observed. Cluster model calculations for the $VO_4^{3-}$ ion have been performed by various authors, in various approximations,[4-7] and the energy level diagram proposed by them was used in our analysis of appearance-potential spectra (APS) (Refs. 8 and 9) and electron-energy-loss spectra (EELS) (Ref. 10) of $YVO_4$. No cluster calculations exist for the $V_2O_4^{4-}$ ion, but since it consists of two $VO_4$ tetrahedra that share a

common oxygen atom, we proposed to use the electron structure of the $VO_4^{3-}$ ion as a first approximation in the comparison with the experimental data on $Ca_2V_2O_7$. We recently made such a comparison in the interpretation of low-energy EELS spectra of $Ca_2V_2O_7$.[11] We found there that the width of the forbidden gap in the $V_2O_7^{4-}$ ion is about 5.5 eV, as compared to 4.2 eV in $VO_4^{3-}$. In the present paper, we report on the analysis of the XPS spectra and the edge features in the electron-excited APS and CILS spectra of $Ca_2V_2O_7$.

## II. EXPERIMENT

### A. Sample

The $Ca_2V_2O_7$ sample material was prepared from stoichiometric amounts of calcium acetate $[Ca(CH_3COO)_2]$ and ammonium vanadate $(NH_4VO_3)$. These ingredients were dissolved in hot water and filtered. A precipitate was obtained by mixing the hot solutions. The highly amorphous precipitate was coagulated by adding concentrated ammonia to the solution. The precipitate was washed, dried at 100°C, and heated for 2 hours at about 700°C. The sample obtained was ground and studied by x-ray diffraction. A thermogravimetric measurement in the temperature range 0–800°C showed no measurable weight loss due to water release, which means that the sample consisted of the pure $Ca_2V_2O_7$ phase and not the divanadate dihydrate $(Ca_2V_2O_7 \cdot 2H_2O)$ phase. The powder material was supported without any glue on a substrate of aluminum in CILS and copper in APS, and pressed into indium in XPS.

### B. Equipment and measurements

The CILS spectra were measured with a PHI-545 scanning Auger-electron spectrometer with a cylindrical mirror analyzer CMA (15-110A). The XPS spectra were measured with a VG-ESCA3 $Mk$II electron spectrometer with monochromatized Al $K\alpha$ excitation radiation. The APS spectra were excited by a quasimonochromatic beam (~4 mA) of electrons emitted by a $V$-shaped tungsten filament.

The vacuum level during the measurements was about $10^{-7}$ Pa in CILS and APS, and $10^{-8}$ Pa in XPS. No charging effect was observed in CILS and APS, while a correction of −1.8 eV was applied to the binding energies measured in XPS. This correction was estimated as the energy distance between the two measured carbon $1s$ component lines arising from carbon contamination on the conductive indium substrate and the insulating sample embedded in it.

The CILS and APS spectra were recorded in the first derivative mode by using usual lock-in amplification technique with a modulation amplitude of 1 V (peak-to-peak) in CILS, and 1.5 V (peak-to-peak) in APS. The measured CILS spectra were thereafter computer integrated and differentiated, in order to evaluate the background below the ionization edge (in the integral spectrum), and to locate accurately the spectral features (in the spectrum of second derivative). The true characteristic ionization-loss features were separated from the Auger lines by comparing the spectra measured at various incident energies. In CILS we used rather high incident electron energies (700–1500 eV) to assure that, upon lifting the core electrons into the lowest available empty states, the incident electrons did not remain in the vicinity of the excited atoms. The price paid for this condition, which is necessary in order to probe the simple density-of-states (DOS) distribution and not its self-convolution, is the rather poor resolution of the experiment resulting mainly because of the large width of the incident electron beam (about 4 eV at 700 eV, 6 eV at 1000 eV, and 9 eV at 1500 eV).

In our experiments, prolonged electron bombardment resulted in a discoloration of the $Ca_2V_2O_7$ sample material in both CILS and APS. No significant modification of the CILS features could be observed, but the shape of the APS spectra changed appreciably, as will be shown in Sec. III C below. In the APS experiment, we also performed argon ion bombardment which resulted in similar effects.

## III. RESULTS AND DISCUSSION

### A. CILS spectra

To illustrate the CILS data, we show in Figs. 1–5 a set of spectra measured at different incident electron energies (740, 1000, and 1500 eV) in which the excitation or ionization of Ca $2p$, V $2p$, and O $1s$ levels appears either isolated or close to some characteristic Auger lines. The shape of the CILS features in these selected spectra illustrates qualitatively the energy variation of the cross section for core level excitation or ionization. What we in fact measured is the differential cross section at the given reflection angle determined by the geometry of the spectrometer (42°), integrated over the angular resolution of the analyzer. The conditions of our experiment did not permit us to perform a detailed quantitative analysis of the energy dependence of these differential cross sections. Figures 6 and 7 show the change with energy of the shape of the CILS spectra, corrected for the back-
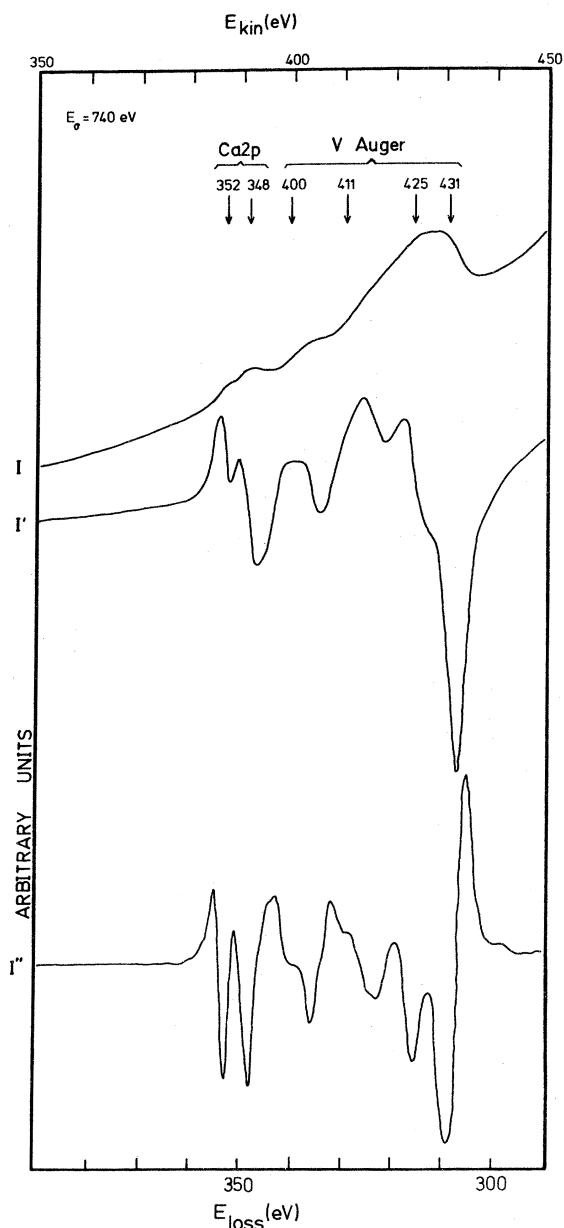
FIG. 1.   CILS spectrum of Ca $2p$ levels in $Ca_2V_2O_7$ at 740-eV incident electron energy.



FIG. 2.   CILS spectrum of V $2p$ and O $1s$ levels in $Ca_2V_2O_7$ at 740-eV incident electron energy.

ground as shown in more detail below. The Ca $2p$ and V $2p$ doublets are better resolved at low incident energy where the resolution is higher. Significant over the entire energy range is the variation of the relative intensity of the Ca $2p$ and V $2p$ doublet lines. The curves in Figs. 6 and 7 cannot be compared quantitatively because their intensity scales are arbitrary and different.

Remarkable also is the behavior of the oxygen structure. It only appears as a weak undulation at 740 eV (curve a), blows up strongly at 1000 eV (curve b), and is almost completely washed
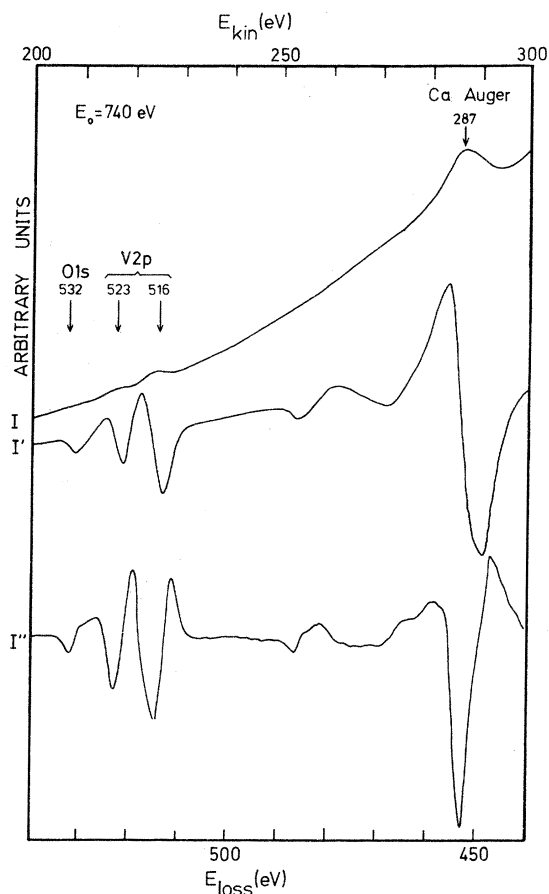
out at 1500 eV. We do not have a good understanding of this behavior. The curves in Figs. 6 and 7 should, however, be considered with suspicion, since the poor knowledge of the shape of the subtracted background might have resulted in some kind of deformation of the final spectra.

The edge side of the ionization curve is sharper at lower incident energies, while its extended tailing at higher incident energies is certainly an artifact introduced by the larger width of the incident beam. For the analysis of the edge shape of the ionization losses, the spectra in Figs. 6(a) and 7(a) were chosen. A portion of the background below the ionization edge (in the integrated spectra) was extrapolated linearly beyond the edge and subtracted from the measured spectra. The true ionization loss spectra $I_0(E_{loss})$ obtained in this way are shown in Figs. 8 and 9, together with their derivative $dI_0/dE_{loss}$. The widths ($l_{Ca}$ and $l_V$) of the edge side of the spectra were determined as the energy distance between the first two zeros in the $dI_0/dE_{loss}$ distributions. All these data are collected in Table I.
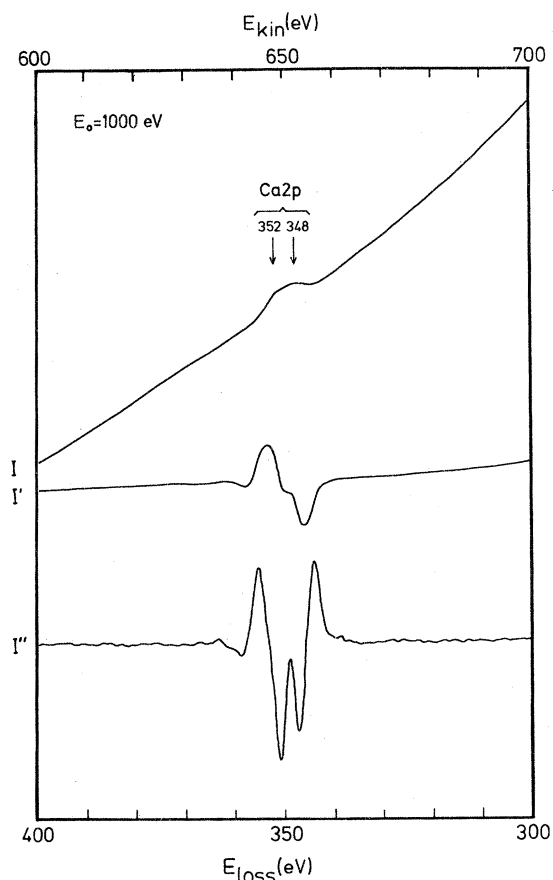
FIG. 3. CILS spectrum of Ca $2p$ levels in $Ca_2V_2O_7$ at 1000-eV incident electron energy.



FIG. 4. CILS spectrum of V $2p$ and O $1s$ levels in $Ca_2V_2O_7$ at 1000-eV incident electron energy.

## B. Comparison of CILS and XPS data

Figures 10 and 11 show the XPS spectra in the region of binding energies of Ca $2p$, V $2p$, and O $1s$ levels. The binding energies and linewidths are given in Table I. We will assume that the excitation of vanadium and oxygen core electrons occurs within the ionic complex $V_2O_7^{4-}$.

Since the core-level binding energies measured in XPS are referenced to the Fermi level of the sample (which is assumed to lie in the middle of the forbidden gap), we can draw a diagram of the electronic states in the $V_2O_7^{4-}$ ion as shown in the left-hand part of Fig. 12. The gap width of 5.5 eV is known from the analysis of low-energy EELS spectra reported earlier by us.[11]

It is seen that the edge of the CILS spectrum, which represents electron transitions from the V $2p_{3/2}$ core level to the lowest available empty state, is lower than the binding energy of the V $2p_{3/2}$ level measured in XPS. The first maximum in the CILS spectrum, which represents transitions from the V $2p_{3/2}$ core level to a higher empty state corresponding to the maximum den-
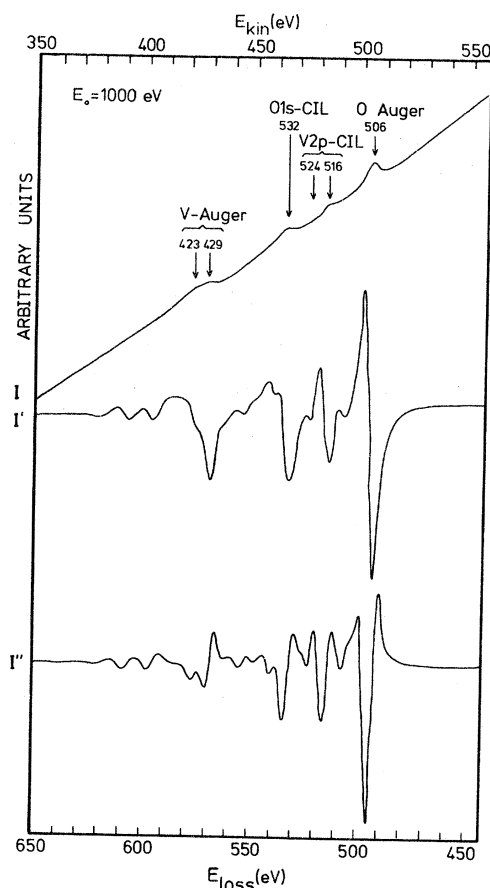
sity of states above the Fermi level, is also lower than the XPS V $2p_{3/2}$ binding energy. The second maximum in the CILS spectrum, corresponding to transitions from the V $2p_{1/2}$ core level to empty molecular orbitals of maximum density, is again lower than the V $2p_{1/2}$ binding energy. These transitions are illustrated in the central diagram of Fig. 12. We also included in this figure the excitation transitions from O $1s$ core levels, although neither their edge nor their maximum could be determined from our CILS spectra.

The diagram in Fig. 12 illustrates how creation of a hole on a deep core level triggers a re-distribution of the outer electronic states. The molecular orbitals are pulled down, even below the Fermi level, at the local site of the excited $V_2O_7^{4-}$ cluster. Assuming that in this re-adjust-ment process the width of the gap is preserved (which means that the molecular orbitals, both occupied and empty, are equally shifted), we estimated the final-state position of the highest occupied valence orbital, the mid-gap-point, the
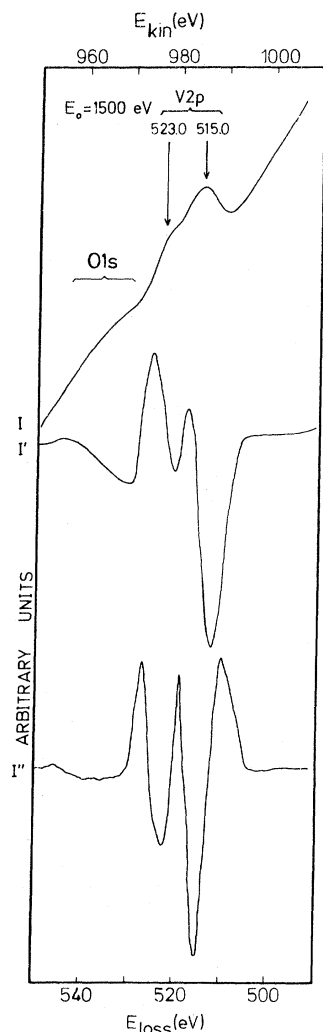
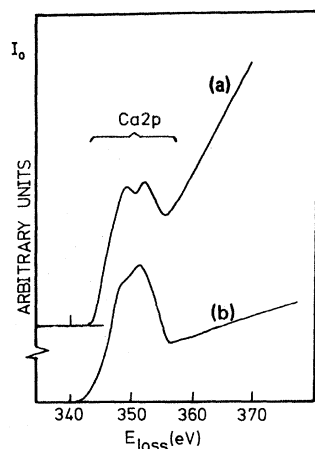FIG. 5. CILS spectrum of V $2p$ and O $1s$ levels in Ca$_2$V$_2$O$_7$ at 1500-eV incident electron energy.



FIG. 6. CILS spectra of Ca $2p$ levels in Ca$_2$V$_2$O$_7$ at various incident electron energies: (a) 740 eV, (b) 1000 eV, after background subtraction.



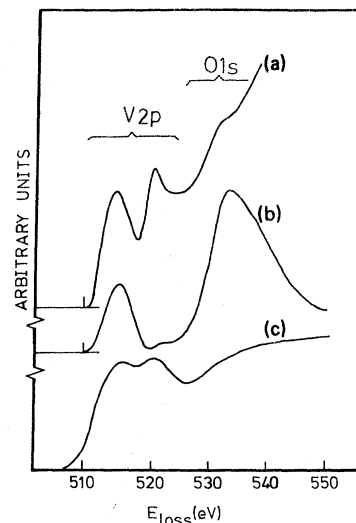FIG. 7. CILS spectra of V $2p$ and P $1s$ levels in Ca$_2$V$_2$O$_7$ at various incident electron energies: (a) 740 eV, (b) 1000 eV, (c) 1500 eV, after background subtraction.

lowest antibonding orbital, and that of maximum density as indicated in the diagram of Fig. 12. This is certainly a crude evaluation that should be refined by further detailed studies. Analysis of $L_{3,2}$ x-ray emission and $L_{3,2}$ $VV$ Auger spectra would be valuable. These spectra would hopefully provide information on the filling of $L_{3,2}$ core holes by radiative or nonradiative transitions, either back from the newly populated antibonding states or from the bonding valence orbitals below the gap. The selection rules operating in x-ray emission spectroscopy (XES) might also reveal
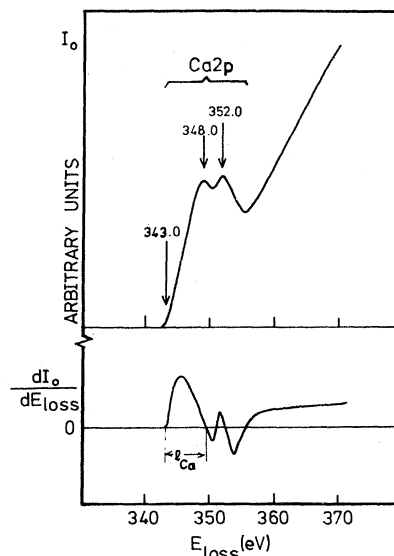


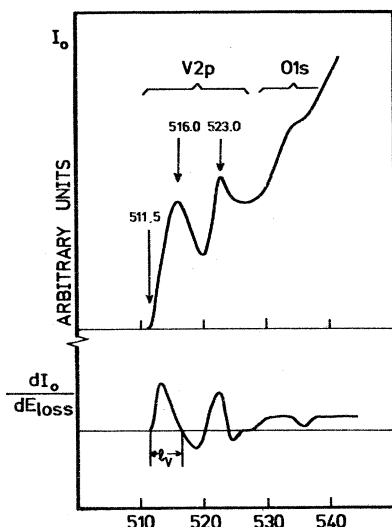FIG. 8. Analysis of the edge side of Ca $2p$ ionization-loss spectrum.

FIG. 9. Analysis of the edge side of V $2p$ ionization-loss spectrum.

the symmetry structure of the molecular orbitals involved. Participation of the initially empty states in the subsequent x-ray emission would appear as an extra feature on the high-energy side of the main maximum in the XES spectra, similar to that observed in $YVO_4$ (Ref. 12) and $V_2O_5$.[13,14] At high enough incident electron energies, two different competing channels exist for the population of the antibonding orbitals. One of them would involve capture of the core electrons directly lifted to the empty orbital at minimum-energy transfer from the incident electrons. The second would involve emission of the core electron into the vacuum at high-energy transfer from the incident electrons, followed by a pulling down of the empty orbitals below the Fermi level, and
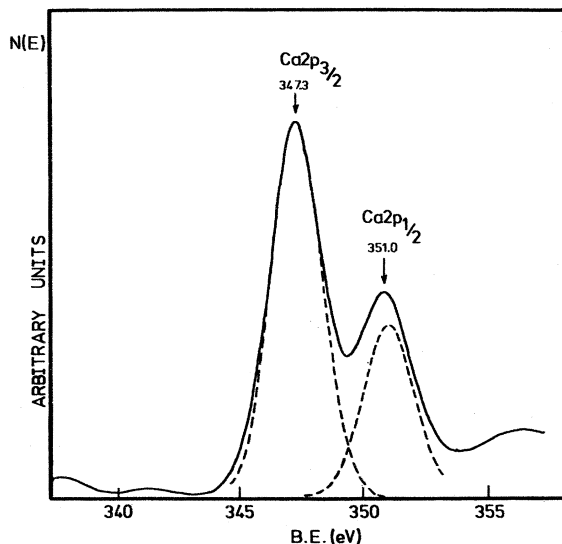


FIG. 10. XPS spectrum of Ca $2p$ levels in $Ca_2V_2O_7$. The component lines were separated by computer analysis of the measured spectrum.

filling of these orbitals by charge flow from the surrounding valence orbitals. An analysis of Auger electron and x-ray emission spectra of $Ca_2V_2O_7$ is now in progress. Decay of the O $1s$ holes might be better suited for study than their creation which appears so badly defined in our CILS data.

The analysis of CILS spectra of calcium is less fruitful. It is believed that excitation of calcium occurs within its own ionic states, outside the $V_2O_7^{4-}$ ion. Calculations of the energy levels of the $Ca^{2+}$ ion are not available. In the CILS spec-
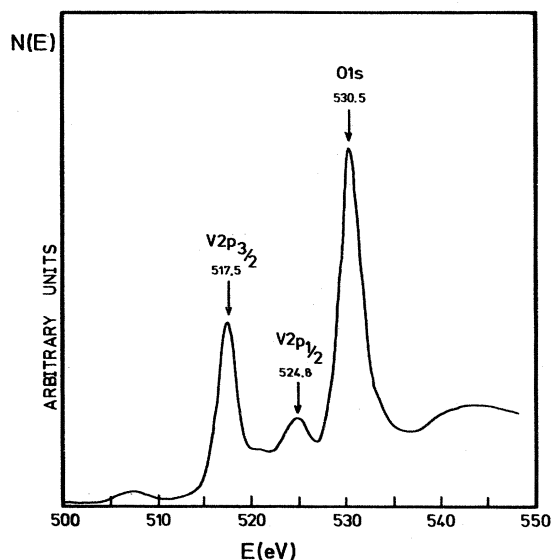
TABLE I. CILS, XPS, and APS data on Ca $2p$, V $2p$, and O $1s$ levels in $Ca_2V_2O_7$.

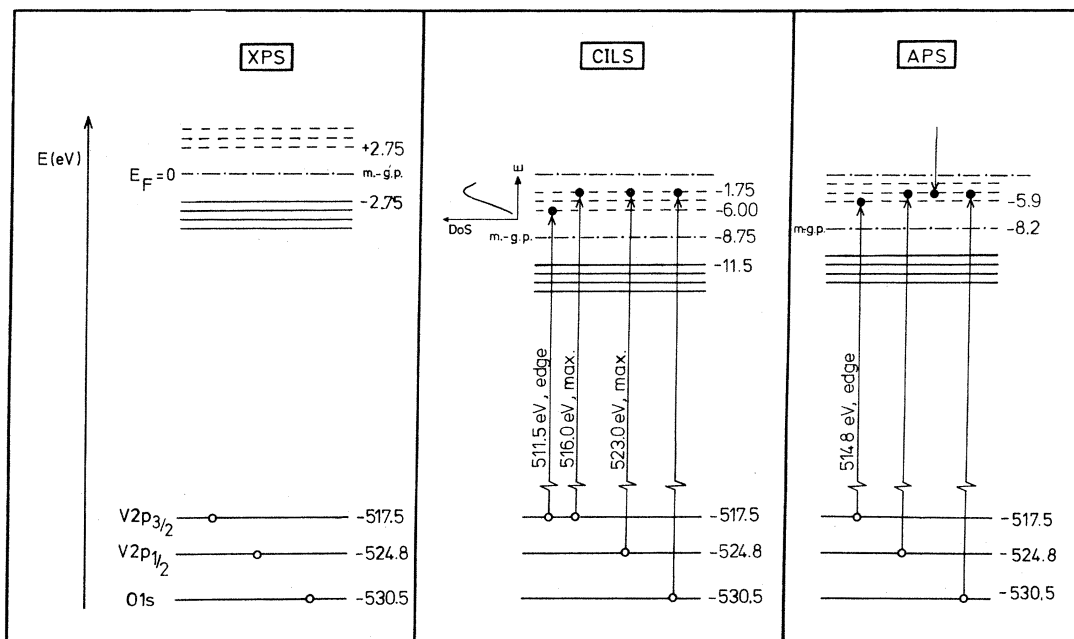| Level | Spectral feature | CILS | Method XPS | APS |
|---|---|---|---|---|
| Ca $2p_{3/2}$ | Edge | 343.0 | | |
| | Maximum | 348.0 | 347.3 | |
| | Edge width | 6.4 | | |
| | Line width | | 5.2 | |
| Ca $2p_{1/2}$ | Maximum | 352.0 | 351.0 | |
| | Line width | | 4.8 | |
| V $2p_{3/2}$ | Edge | 511.5 | | 514.8 |
| | Maximum | 516.0 | 517.5 | 518.6 |
| | Edge width | 4.8 | | |
| | Line width | | 2.7 | |
| V $2p_{1/2}$ | Maximum | 523.0 | 524.8 | 525.8 |
| | Line width | | 3.0 | |
| O $1s$ | Edge | (?)528.5 | 530.5 | |
| | Line width | | 3.0 | |



FIG. 11. XPS spectrum of V $2p$ and O $1s$ levels in $Ca_2V_2O_7$.

FIG. 12. Energy-level diagrams of the electronic states in $Ca_2V_2O_7$, as deduced from XPS, CILS, and APS data.

tra, the $Ca\,2p_{3/2}$ edge and the $Ca\,2p_{3/2}$ and $Ca\,2p_{1/2}$ maxima are well defined. We observe that the $Ca\,2p$ CILS maxima are somewhat higher, but very close to the $Ca\,2p$ binding energies measured in XPS, while the $Ca\,2p_{3/2}$ edge is about 4.5 eV lower than the $Ca\,2p_{3/2}$ XPS binding energy. It seems as if the $Ca\,2p$ core hole is more efficiently (or completely) screened as compared with the $V\,2p$ hole, or alternatively that the final state is gone into the continuum. The edge width of the

$Ca\,2p_{3/2}$ CILS spectrum (6.4 eV) is higher than that of the $V\,2p_{3/2}$ spectrum (4.8 eV).

## C. APS spectra

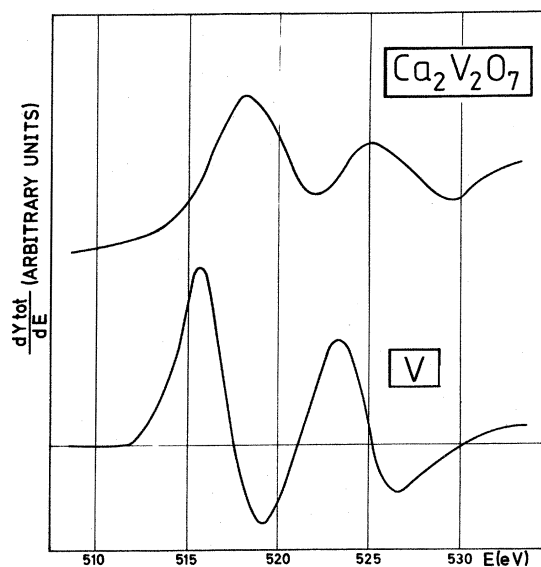Figure 13 shows the $V\,2p$ APS spectrum of $Ca_2V_2O_7$, together with that of pure vanadium



FIG. 13. APS spectrum of $V\,2p$ levels in $Ca_2V_2O_7$ (this work) and in pure vanadium (Ref. 15).
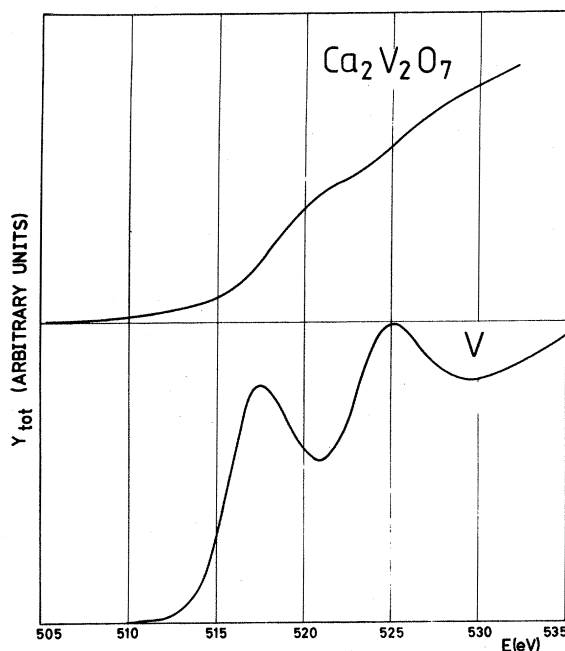


FIG. 14. The spectra of total soft x-ray emission yield, obtained through integration of the spectra in Fig. 13.
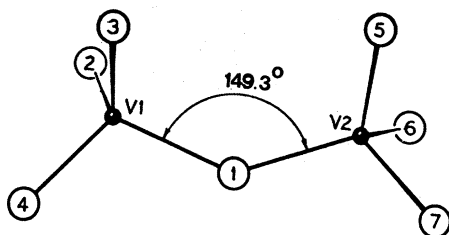
FIG. 15.  V-O coordination within the $V_2O_7$ cluster in $\alpha$-$Zn_2V_2O_7$.
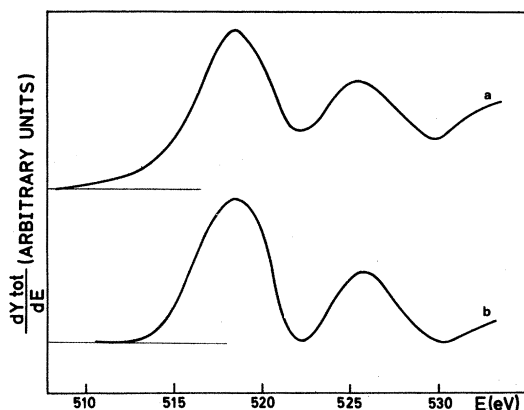


FIG. 16.  The V $2p$ derivative APS spectra of $Ca_2V_2O_7$ in the "as received" state (a), and after prolonged electron bombardment (b) ($\sim$2 h, 500 eV, 4 mA).

taken from the work of Park and Houston.[15] The position and shape of these spectra are significantly different as a result of both the shift of the V $2p$ core levels and the modification of the electron structure of the empty states when passing from elementary vanadium to the vanadium compound. Most striking is the fact that the APS spectrum of $Ca_2V_2O_7$ does not display the negative undershoot characteristic for materials that have high density of empty states confined within a narrow energy interval above the Fermi level. This aspect is better illustrated by the integrated spectra of total soft x-ray emission yield shown in Fig. 14. It is seen that the $L_3$ and $L_2$ features only appear as undulations in the drastically increasing yield, the resonant character of the APS processes being almost completely lost. This is a measure of the delocalization of the empty orbitals in the $V_2O_7$ cluster. The smearing out of the V $2p$ APS spectra of $Ca_2V_2O_7$ is more pronounced than of those of $YVO_4$,[8] which means that the broadening and delocalization of orbitals is higher. This is consistent with the crystal structure data on these compounds, which indicate a much larger spatial extension of the $V_2O_7$ cluster than that of the $VO_4$ cluster. In $YVO_4$, vanadium is tetrahedrally coordinated to oxygen to form the $VO_4^{3-}$ anion.[16] The crystal structure of $Ca_2V_2O_7$ is not exactly known, but it is believed to be similar with that of $\alpha$-$Zn_2V_2O_7$, for which Gopal and Calvo have given a detailed description.[17] Both crystals are monoclinic, with the same $\beta$ angle of $\sim$112°. In $\alpha$-$Zn_2V_2O_7$, the anion consists of a pair of $VO_4$ tetrahedra that share a common oxygen atom situated on a twofold axis. The bridging V–O–V bond is non-linear, showing a large bending angle (149.3°) (Fig. 15). The length of the bridging V–O bond is 1.775 Å, while that of the three independent terminal ones is 1.728, 1.704, and 1.658 Å. The assumption that $Ca_2V_2O_7$ is isomorphous with $\alpha$-$Zn_2V_2O_7$ is supported by the similarity of their luminescent spectra [the maximum of the luminescent band is at 700 nm for $Ca_2V_2O_7$,[18] and at

650 nm for $Zn_2V_2O_7$ (Ref. 19)]. It also is consistent with the difference in density, taking into account the differences in atomic weights and ionic radii of the cations.

The values of the edge and maxima in our measured V $2p$ APS spectra of $Ca_2V_2O_7$ are given in Table I, and they are remarkably close to those measured by us for $YVO_4$.[8] The maxima in the APS spectra are in fact the "second structures" arising from the self-convolution of the density of empty states involved in the APS processes.[15] The "first structure," which should be located at the energy position of these states, could not be resolved in our spectra. The reason may be the poor resolution of our experiment (we used modulation amplitudes of $\sim$1.5 eV to detect the derivative spectra), but certainly also the shape of the orbital distribution above the Fermi level. (If the width of the empty states is comparable to, or larger than the width of the gap, then the two "structures" will merge into a single one.)
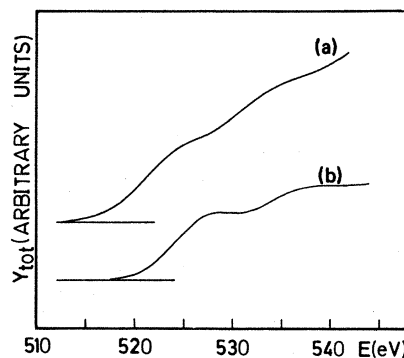


FIG. 17.  The spectra of total soft x-ray emission yield obtained by integration of the curves in Fig. 16.
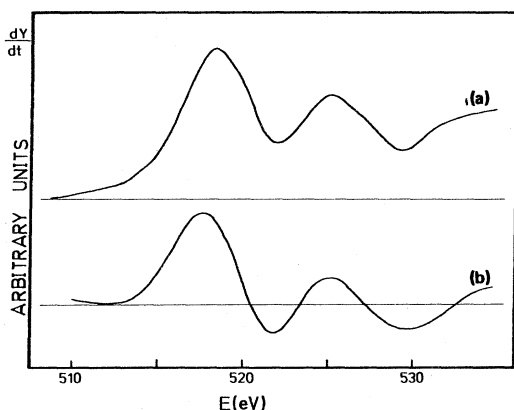
FIG. 18. The V $2p$ derivative APS spectra of $Ca_2V_2O_7$ in the "as received" state (a), and after prolonged argon ion bombardment (b) (~8 h, 1500 eV, ~$10^{-3}$ Pa).



FIG. 19. The spectra of total soft x-ray emission yield obtained by integration of the curves in Fig. 18.

In the APS case too, creation of a core hole on the V $2p$ levels results in a rearrangement of the outer valence and empty orbitals. We illustrate this in the diagram on the right-hand part of Fig. 12. As expected, the situation is different in APS as compared with CILS, since the electronic configurations involved in these processes are different.

Because of its too close proximity to the V $2p_{1/2}$ region, the oxygen APS spectrum could not be analyzed in the present work. Excitation of Ca $2p$ level was not observed. Finally, we mention the modification of the APS spectra observed after prolonged electron and argon ion bombardment. This is illustrated in Figs. 16–19. A slight shift of the maxima is observed in both cases, as is an increased resonance character of the spectral features. No systematic investigation of these effects was done in the present work. We only notice here that they are similar to those observed earlier in $YVO_4$.[8]

## IV. SUMMARY AND CONCLUSIONS

Knowledge of the electron structure of luminescent vanadium-oxygen compounds is essential for the understanding of their properties.
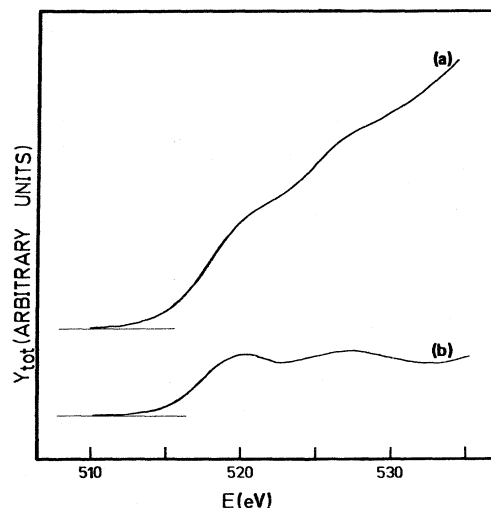
In the absence of detailed theoretical calculations, useful information can be obtained by combining the data provided by various spectroscopic methods. Both excitation with electrons and x rays are interesting, since they reproduce the conditions encountered in the practical use of these materials in cathodoluminescence and radioluminescence.

In the present work we used two electron-stimulated edge spectroscopies, CILS and APS, that probe in different specific ways the structure of the lowest empty states above the Fermi level, and also x-ray photoelectron spectroscopy. Our experimental data are collected in Table I. From the analysis of CILS and APS data on V $2p$ and O $1s$ levels and their comparison with the XPS binding energies, we deduced the energy-level diagram of the $V_2O_7^{4-}$ anion.

Our data illustrate the strong many-body effects that occur in the excitation and decay of localized atomiclike configurations within the big ionic cluster $V_2O_7^{4-}$. The configuration transitions involved in the excitation and decay of V $2p$ levels

TABLE II. Configuration transitions involved in the CILS, APS, and XPS processes in $Ca_2V_2O_7$.

| CILS | | | $2p^6$("empty MO")$^0$ + $e^-$(incident) → $2p^5$("empty MO")$^1$ + $e^-$(∞) |
|---|---|---|---|
| | "1st struct." | Excitation | $2p^6$("empty MO")$^0$ + $e^-$(incident) → $2p^5$("empty MO")$^1$ + $e^-$("itinerant") |
| | | Decay | $2p^5$("empty MO")$^1$ → $2p^6$("empty MO")$^0$ + $h\nu$ |
| APS | "2nd struct." | Excitation | $2p^6$("empty MO")$^0$ + $e^-$(incident) → $2p^5$("empty MO")$^2$ |
| | | Decay | $2p^5$("empty MO")$^2$ → $2p^6$("empty MO")$^1$ + $h\nu$ |
| | | Bremsstr. contrib. | ("empty MO")$^0$ + $e^-$(incident) → ("empty MO")$^1$ + $h\nu$ |
| XPS | | | $2p^6$ + $h\nu$(incident) → $2p^5$ + $e^-$(∞) |

in CILS, APS, and XPS are given in Table II. Similar transition reactions can be written for the excitation of Ca $2p$ levels, and in the same manner for the excitation of O $1s$ levels. However, excitation of calcium, outside the $V_2O_7$ ion, seems to involve more extended orbitals since the screening of its $2p$ core hole was found to be more efficient than for vanadium.

Excitation of Ca $2p$ levels was not observed in APS, but appeared as well defined structures in CILS and XPS. Further studies are necessary, using different other spectroscopic methods. An analysis of Auger electron and x-ray emission spectra of $Ca_2V_2O_7$ is in progress.

[1] R. L. Gerlach, J. Vac. Sci. Technol. **8**, 599 (1971).

[2] R. L. Park, Surf. Sci. **48**, 80 (1975).

[3] A. A. Fotiev, B. V. Shulgin, A. S. Moskvin, and F. F. Gavrilov, *Crystalline Vanadate Phosphors* (Nauka, Moscow, 1976).

[4] W. Walter and K. H. Butler, J. Electrochem. Soc. **116**, 1245 (1969).

[5] V. A. Gubanov, J. Weaver, and J. V. D. Connolly, J. Chem. Phys. **63**, 4 (1975).

[6] V. A. Gubanov, D. E. Ellis, and A. A. Fotiev, J. Solid State Chem. **21**, 303 (1977).

[7] N. I. Lazukova, V. A. Gubanov, M. P. Butzman, V. M. Cherkashenko, E. Z. Kurmaev, and A. A. Fotiev, Zh. Strukt. Khim., **21**, 41 (1980).

[8] I. M. Curelaru and P. O. Nilsson, J. Phys. Chem. Solids **40**, 887 (1979).

[9] I. M. Curelaru and G. Wendin, Phys. Scr. **22**, 513 (1980).

[10] I. M. Curelaru, E. Suoninen, P. Ahlqvist, P. Apell, E. Minni, T. Rönnhult, and K.-G. Strid, Phys. Rev.

B **22**, 4698 (1980).

[11] I. M. Curelaru, E. Suoninen, E. Minni, K.-G. Strid, and T. Rönnhult, *Proceedings of the International Conference on the Physics of Transition Metals* (Leeds, United Kingdom, 1980); Inst. Phys. Conf. Ser. **55**, 153 (1981).

[12] E. Z. Kurmaev, V. M. Cherkashenko, and V. A. Gubanov, J. Electron Spectrosc. Relat. Phenom. **16**, 455 (1979).

[13] D. W. Fischer, J. Appl. Phys. **40**, 4151 (1969).

[14] V. M. Cherkashenko, V. E. Dolgih, E. Z. Kurmaev, and A. A. Fotiev, J. Solid State Chem. **22**, 217 (1977).

[15] R. L. Park and J. E. Houston, Phys. Rev. B **6**, 1073 (1972).

[16] J. A. Baglio and G. Gashurov, Acta Crystallogr. Sect. B **24**, 292 (1968).

[17] R. Gopal and C. Calvo, Can. J. Chem. **51**, 1004 (1973).

[18] B. Henderson and J. E. Wertz, Adv. Phys. **17**, 749 (1968).

[19] I. M. Chaplina, Zh. Prik. Khim. **37**, 1835 (1964).